

# A New Proposed Triple Active Bridge Converter for Fuel Cell Applications: Study, Control and Energy Management

Case Study

## Abdelkarim Aouiti

Computer laboratory for electrical systems,  
LR11ES26, INSAT, University of Carthage,  
Centre Urbain Nord BP 676 - 1080 Tunis Cedex, TUNISIA  
abdelkarim.aouiti.ensit@gmail.com

## Mokhtar Abbassi

Computer laboratory for electrical systems,  
LR11ES26, INSAT, University of Carthage,  
Centre Urbain Nord BP 676 - 1080 Tunis Cedex, TUNISIA  
mok98474304@gmail.com

## Faouzi Bacha\*

University of Tunis, Tunisia  
ENSIT, Ave Taha Hussine, 1008, Tunis  
faouzi.bacha@esstt.rnu.tn

\*Corresponding author

**Abstract** – This paper deals with a new proposed three port converter structure dedicated for two-input source hybrid systems especially for fuel cell applications. This converter is made up of three-phase triple active bridges which are galvanically isolated by means of three single phase high frequency transformers. The present converter integrates a fuel cell as the primary power source with a battery that stores energy, harnessing the unique benefits of both sources to deliver reliable power to a DC load through a single power conversion stage. In order to control the power flow between the ports, a phase shift control technique has been carried out to generate the control signals of the load and battery side bridges in reference with those of the fuel cell bridge. A detailed analysis of the proposed converter has been presented in this paper. A novel proposed energy management algorithm has been developed. This algorithm provides a robust solution for managing and distributing power flow between the converter's ports, ensuring an optimal balance of power delivery. The algorithm has been rigorously validated through simulations and experimental test, using Dspace 1104 board.

---

**Keywords:** Power flow control, three port converter, high frequency transformer, phase shift control technique

---

Received: February 13, 2024; Received in revised form: August 10, 2024; Accepted: August 13, 2024

## 1. INTRODUCTION

Today, global greenhouse gas emissions, primarily from fuel activities, have led to a 1°C rise in the global average temperature since the pre-industrial era. Projections indicate that without intervention, the global average temperature will surpass 1.5° C between 2030 and 2052. The heavy reliance on fossil fuels is unsustainable due to their significant CO<sub>2</sub> emissions and the impending surge in operating costs as reserves dwindle post-2030, [1]. Moreover, global oil reserves, estimated at around 1,732 billion barrels—equivalent to about 52 years of production at current rates—stood

at the end of 2020. This is a theoretical duration, considering that production from existing fields declines over time, amounting to approximately 236,295 million tonnes, [2]. To combat emissions, system designers are exploring cleaner, more efficient energy alternatives, with renewable sources expected to replace fossil fuels over time. Challenges include improving fuel cell efficiency and internal structures. Hydrogen is identified as an ideal energy source, and multi-source hybrid systems, integrating fuel cells with storage batteries and supercapacitors, are proposed to enhance dynamic response to load variations.

Recent renewable energy developments in hybrid systems, aerospace, smart grids, and portable devices have spurred challenges in designing new energy conversion systems. These systems use multi-input power electronic converters to integrate various power sources and provide a well-controlled output for diverse applications. So, converters have evolved from single input/single output to multi-input/multi-output structures, with two reported topologies in the literature [3]. The first topology adopts a conventional structure by consolidating various sources on a common bus. Each source undergoes separate power conversion stages with independent control for each converter. A communication bus facilitates information exchange between sources, leading to increased complexity and higher converter costs due to the involvement of multi-stage power conversion and necessary communication devices. The second multiport topology treats the entire structure as a single power converter, combining multiple sources with power regulation by a centralized controller. These converters, with their simple structure, minimum converter stages, and fewer devices, find applications in various fields, including hybrid power systems, hybrid vehicles, aerospace, satellite applications, portable electronic devices, and uninterruptible power supplies.

Multiport converters are categorized into two types: isolated converters and non-isolated converters. Isolated converters are utilized to separate the low voltage side from the high voltage side, mitigating the risk of electric shock and ensuring voltage compatibility. Additionally, achieving a high voltage output necessitates the inclusion of an isolation stage in converters for upcoming power conversion systems. Galvanic isolation using high-frequency (HF) transformers is imperative for these systems due to several advantages. They offer compact size, lightweight, and cost-effectiveness. Moreover, they significantly reduce noise and minimize the size of passive elements due to their high switching frequency. Furthermore, HF transformers prevent harmonic current and voltage distortions induced by the saturation of low-frequency transformer cores.

In this context, this article presents a recent trend in the development of a converter dedicated for a multi-source hybrid system. Through this work, we propose a new multiport converter topology. This structure uses three-phase three port active bridge DC-DC converters in order to benefit from the advantage of the elementary DAB-3ph structure and the three-phase configuration. In fact, the three-phase double active bridge reveals the following benefits: low electromagnetic interference due to high frequency operation, the compactness of the transformer size, the minimized effective currents through the switches and diodes, and a greatly reduced conduction losses with an inherent smooth switching of power switches, [4, 5].

The single-phase and the three phase DAB have both been firstly proposed in [6]. The characteristics of the materials and components, particularly the significant

losses brought on by the low frequency transformers, severely constrained the benefits of these converters.

After the development of the power converter components and the improvement of the core materials, the literature has shown a significant interest in the single-phase [7-14] and three-phase double active bridge [3, 4] configurations, and several works have been presented. Also, the elementary dual active bridge structure has been extended to accommodate three ports. A triple active bridge converter is proposed in [15-17]. While [15] focuses on electric vehicle charging, utilizing a generalized-harmonic-approximation method for accurate waveform prediction and achieving high efficiency (97.6%) with zero-voltage switching, [16] emphasizes ZVS across a wide load range and input voltage. In [17], a decoupling control method for a triple active bridge has been introduced, enabling simultaneous charging of two EV battery stacks while maintaining isolation.

In [18], a 3p-3ph converter for high-power applications integrates a slow transient main energy source and a fast storage device to supply a DC load. Using three bidirectional full bridge inverters and a 3p-3ph high-frequency transformer, power flow is controlled by adjusting phase shift angles among the inverter stages. While this structure offers the advantage of handling three ports, it faces limitations related to voltage level capability. In [19], a fuel cell-powered uninterruptible power supply system integrates a three-port bidirectional converter, linking the fuel cell and supercapacitor to a grid-connected inverter. It operates in stand-alone or grid-connected modes, with two bridge phase shifts controlling the DC/DC stage for simultaneous adjustment of fuel cell power and DC-link voltage. However, this structure is noted for its high current distortion compared to the three-phase structure and its low output voltage level. As to [20], a novel three-port bidirectional converter with a three-winding coupled inductor is proposed for PV systems, enabling high step-up/step-down conversion. In [21], a novel approach to integrate hybrid energy storage systems (HESSs) with renewable energy sources (RES) and loads using a current-fed dual active bridge (DAB) converter has been proposed. This method regulates load voltage, tracks RES maximum power point, and safeguards the battery from transients, enhancing system efficiency and reliability.

In this work, a novel three-port converter topology is proposed. By integrating the three-phase triple active bridge structure with the buck-boost configuration, this converter offers a solution that combines the advantages of both topology and overcomes the lack of the voltage level for the three-port configuration. This converter accommodates a fuel cell which represents the main source in the system; and a battery which allows energy storage. The advantages of the two sources are combined in order to supply a DC load while using a single conversion stage. The instantaneous power in the system can be distributed in a controlled way, which improves its dynamics and it increases its reli-

ability. This multiport converter is intended for medium to high power applications. Its main characteristics is the combination of three galvanically isolated ports with bidirectional power flow capabilities; where the voltage of the main source could be raised thanks to the employment of a boost structure, so a wide input voltage range could be applied and the gain could be adjusted by the duty cycle of switches of the principal bridge. The power flow in this system is simple, it may be achieved by introducing two phase shift angles. Moreover, the converter uses tiny passive elements, and it has very low current ripples. So, the system exhibits low power losses and important conversion efficiency. The principle of operation, as well as the control strategies adopted for the proposed converter, have been studied in details. A novel energy management algorithm has been developed to facilitate efficient and balanced power flow among the ports of the three-port converter. The algorithm's effectiveness in improving converter efficiency and power management was demonstrated through comprehensive simulations and experimental tests utilizing Dspace 1104 board.

## 2. SYSTEM DESCRIPTION

Fig.1 shows the proposed three port converter topology. This circuit is an extension of the three-phase DAB topology and thereby it is called a three-phase triple active bridge (TAB) converter. It is composed of three single-phase transformers with two secondaries. On the low voltage side, an interleaved boost structure is used to raise the voltage of the fuel cell. The boost mode is carried out by the inductors  $L_{dc1}$ ,  $L_{dc2}$  and  $L_{dc3}$  and the three half-bridges of the low voltage side; and this to keep constant the voltage of the DC bus of port 1 and in order to allow a wide range for the variation of the fuel cell voltage. For the high voltage side, a load is connected to the first output port. As for the second output port, a battery, which acts as an energy storage device, is connected. The converter can operate in step-up mode when power is flowing from the low voltage side (LVS)

to the high voltage side (HVS) in order to supply the load and / or charge the battery. A transfer of power is also permitted from the battery to the load.

The switches of the three bridges are switched at the same frequency and these bridges generate the voltages  $v_{an}$ ,  $v_{rM1}$  and  $v_{oM2}$  having a controlled phase shift with respect to the primary side ( $v_{an}$ ). The maximum allowed power flow between the ports is directly related to the external inductances.

The three-phase triple active bridge (TAB) converter proposed in this study offers several significant advantages, making it an ideal solution for high power applications. In fact, it enables the combinations of three ports, including a high output voltage for the load through boosting the voltage of the main source. Moreover, the converter features a simple power flow control owing to the application of the phase shift control technique, effectively reduces current ripples.

The use of small-sized passive elements is made possible by the application of a high frequency galvanic isolation between the three ports.

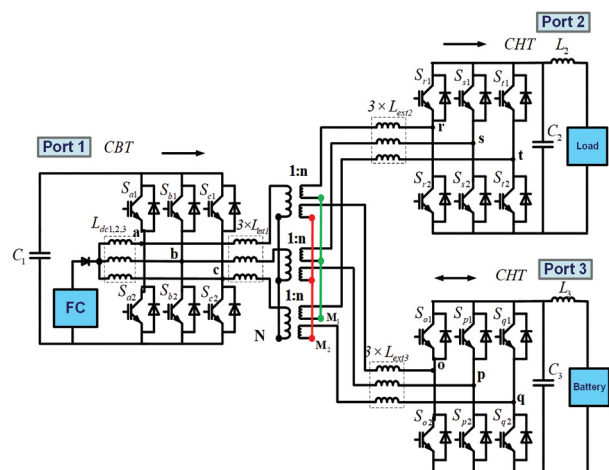


**Fig. 1.** Three-port three-phase active triple bridge converter diagram

**Table 1.** Comparison Table between the proposed converter and the existing topologies in the literature

Topology	Dual Active Bridge Multiport converter [21]	Three-port Bidirectional DC-DC converter [17]	Three-Port Three-Phase DC-DC Converter [18]	Proposed converter
<b>Criteria</b>				
Bidirectional power flow	✓	✓	✓	✓
Power (W)	135	5x103 (x 2 output)	103	10x103
Fully Isolated ports	x	✓	✓	✓
Output voltage (V)	100	400 (x 2 output)	800	200
Switching frequency (kHz)	50	20	100	20
Number of bridges / legs	2 briges and one leg	3	3	3
Number of switches	10	12	18	18
Power flow control	Phase shift control / Duty cycle	Phase shift control	Phase shift control	Phase shift control
Focus	Operation and control	Control	Control and transformer design	Energy management
Application	Renewable energy application	Electrical vehicle battery charging	Grid connected	Electrical Vehicle

The proposed converter exhibits exceptional bidirectional power flow capabilities and high-power density. With its compact size and fully isolated ports, it guarantees superior safety and reliability in operation.

Additionally, the converter provides a high output voltage at its output, significantly expanding its applicability across diverse tasks

Table 1 highlights the unique features and advantages of the proposed three-port converter in contrast to the existing topologies in the literature. It emphasizes the converter's versatility, efficiency, and reliability across various applications, particularly its suitability for electric vehicles and hybrid systems.

### 3. CONTROL STRATEGY AND DIFFERENT OPERATING MODES OF THE PROPOSED CONVERTER

A full wave control is chosen for the transformer primary-side inverter. As to the other bridges, a phase shift control has been adopted. So, the control signals could be expressed as:

$$\begin{cases} S_{j1}(\theta) = S_{r1}(\theta - \varphi_{12}), (i, j) = \{(a, r), (b, s), (c, t)\} \\ S_{k1}(\theta) = S_{r1}(\theta - \varphi_{13}), (i, k) = \{(a, o), (b, p), (c, q)\} \\ S_{m2} = \overline{S_{m1}}, m = \{a, b, c, r, s, t, o, p, q\} \end{cases} \quad (1)$$

Fig. 2 shows the  $\Delta$ -model of the system where the three bridges are replaced by three voltage sources  $v_{ant}$ ,  $v_{rM1}$  and  $v_{oM2}$ . The sources exchange energy through a network of inductors. The voltages  $v_{rM1}$  and  $v_{oM2}$  are respectively shifted by  $\varphi_{12}$  and  $\varphi_{13}$  with respect to the reference voltage van. The phase shifts are considered positive when the corresponding voltage is lagging in phase with respect to the reference van and they are negative when the considered voltage is leading the reference voltage van.

The inductors of  $\Delta$ -model are derived from the transformer leakage inductors and the inductors  $L_{ext1}$ ,  $L_{ext2}$  and  $L_{ext3}$ . Using this representation, the three-port system is broken down into three two-port subsystems which facilitates its analysis and its modelling. The magnetizing inductance, which does not contribute to the power flow, is neglected to simplify the analysis and therefore it is not shown in Fig. 2. According to the definitions of the  $\Delta$ -model of Fig. 2 where all the quantities are brought back to the transformer primary-side, the relation between the phase shift angles and the power flow in the system turns out to be as follows:

$$P_{ij}(\varphi_{ij}) = \begin{cases} \frac{V_i V_j}{n L_{ij} \omega} \varphi_{ij} \left( \frac{2}{3} - \frac{\varphi_{ij}}{2\pi} \right) \text{ for } 0 \leq \varphi_{ij} \leq \frac{\pi}{3} \\ \frac{V_i V_j}{n L_{ij} \omega} \left( \varphi_{ij} - \frac{\varphi_{ij}^2}{\pi} - \frac{\pi}{18} \right) \text{ for } \frac{\pi}{3} \leq \varphi_{ij} \leq \frac{2\pi}{3} \end{cases} \quad (2)$$

Where,  $V1 = V_{FC}$ ,  $V2 = V_{load}$  et  $V3 = VBT$  are the voltages at the ports; and  $\varphi_{ij}$  presents the phase shifts in radians and n denotes the transformation ratio of the transformer.

The phase shifts  $\varphi_{ij}$  are selected according to the powers that should be transferred between the ports. Taking into account the expressions of the powers  $P_{ij}$  between a port "i" and a port "j", the maximum power flow through  $L_{ij}$  occurs for the value  $\pi/2$  of the phase shift angle. Once the inductors  $L_{ij}$  are fixed, the inductors  $L_{ext1}$ ,  $L_{ext2}$  and  $L_{ext3}$  are determined by the  $\Delta$ -T transformation and using equations presented in appendices 1.

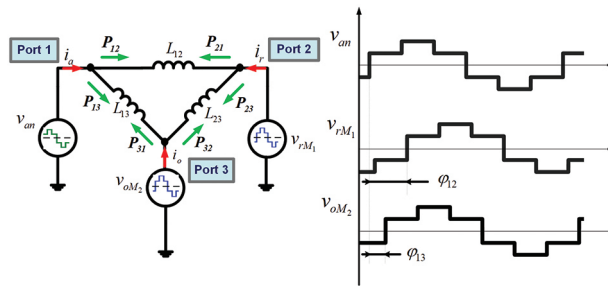


Fig. 2. Three-port three-phase active triple bridge converter diagram

Using the  $\Delta$ -model in Fig. 2, the power flow at each port is a combination of the power flows through two associated branches. For a lossless system, they are:

$$\begin{cases} P_1 = P_{12} + P_{13} \\ P_2 = -P_{12} - P_{32} \\ P_3 = P_{32} - P_{13} \\ P_1 + P_2 + P_3 = 0 \end{cases} \quad (3)$$

Where  $P_1 = P_{FC}$  is the power supplied by port 1 (the main source  $P_{FC}$ ) to port 2 and port 3,  $P_2 = -P_{Load}$  is the power supplied to the port 2 (the charge port) (a negative sign of  $P_2$  means that the load consumes energy) and  $P_3 = P_{BAT}$  is the power drawn from port 3 (the storage port) (a negative sign of  $P_3$  implies that the energy is stored in the battery).

The parameters of the proposed converter are given by the following table:

Table 2. Parameters of the three-port three-phase active triple bridge converter

Parameters	Designation	Value
$L_{dc1}-L_{dc2}-L_{dc3}$	Boost Inductance	1.2 $\mu$ H
$L_{ext1}$	Primary side external inductance	1.35 $\mu$ H
$L_{ext2}$	1st Secondary side external inductance	12.9 $\mu$ H
$L_{ext3}$	2nd Secondary side external inductance	26.3 $\mu$ H
n	Transformation ratio of the transformer	7
fs	Switching frequency	20 kHz

By controlling the phase-shift angles between the three ports, the three-port converter operating modes can be distinguished by the combination of power flows. Since the fuel cell cannot absorb power, there are only six modes as follows:

Mode 1: the fuel cell supplies the DC load and simultaneously charges the battery.

Mode 2: the load is supplied by both sources at the same time: the fuel cell and the battery.

Modes 3: the load is only supplied by the fuel cell.

Modes 4: the load is only supplied by the battery.

Mode 5: only concerns battery charging via the fuel cell.

Mode 6: No power transit between the ports.

**Table 3.** The possible operating modes according to the power flow combinations

Load power	Battery power	Fuel cell power	
		$P_{FC} > 0$	$P_{FC} = 0$
$P_{Load} < 0$	$P_{BAT} > 0$	Mode 2	Mode 4
	$P_{BAT} < 0$	Mode 1	Doesn't exist
	$P_{BAT} = 0$	Mode 3	Doesn't exist
$P_{Load} = 0$	$P_{BAT} > 0$	Doesn't exist	Doesn't exist
	$P_{BAT} < 0$	Mode 5	Doesn't exist
	$P_{BAT} = 0$	Doesn't exist	Mode 6

The selection of the convenient mode is according to the load demand and the state of the charge of the battery. Once the mode is selected, the reference powers are provided and after that the phase shift are determined, as illustrated by Fig. 3 and table 4.

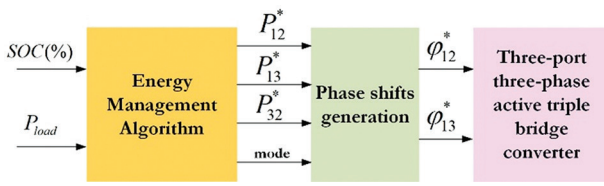


**Fig. 3.** Energy management and phase shift angles generation for the three-port three-phase active triple bridge converter

**Table 4.** The different operating modes as function of the phase shift angles  $\varphi_{12}$  and  $\varphi_{13}$

Mode	$\varphi_{12}$ (rad)	$\varphi_{13}$ (rad)
Mode 1	$0 < \varphi_{12} \leq \pi/2$	$\varphi_{13} = \varphi_{12}$
Mode 2	$0 < \varphi_{12} \leq \pi/2$	$\varphi_{12} < \varphi_{13} \leq 2\pi/3$
Mode 3	$0 < \varphi_{12} \leq \pi/2$	$\varphi_{12}/2$
Mode 4	0	$(-\pi)/2 \leq \varphi_{13} < 0$
Mode 5	0	$0 < \varphi_{13} \leq \pi/2$
Mode 6	0	0

#### 4. ENERGY MANAGEMENT

An energy management algorithm for the three-port converter has been proposed to manage the power flow in the system. This energy management algorithm, which is shown by Fig. 4, aims to optimize the power flow between the fuel cell, battery, and load in order to maximize the efficiency and longevity of the system. By monitoring the state of charge of the battery, the power demand of the load, and the output power of the fuel cell, the algorithm can dynamically adjust the power flow to maintain a balance between the different components and ensure that the load is always receiving the required amount of power.

To assess the power distribution strategy's effectiveness and observe system behavior across various modes of operation, we employed a load profile and battery state of charge as depicted in Fig. 5. The load

power, which is depicted in blue, varies between 0 and 1200 W, reflecting typical real-world operating conditions that test the system's ability to adapt dynamically to fluctuating power demands. Meanwhile, the state of charge, shown in green, ranges from 20 to 100%. The fuel cell provides 1200 W and the battery offers 1000 W. Figs. 6 and 7 illustrate the transferred powers and power distribution across the ports for both experimental and simulation tests.

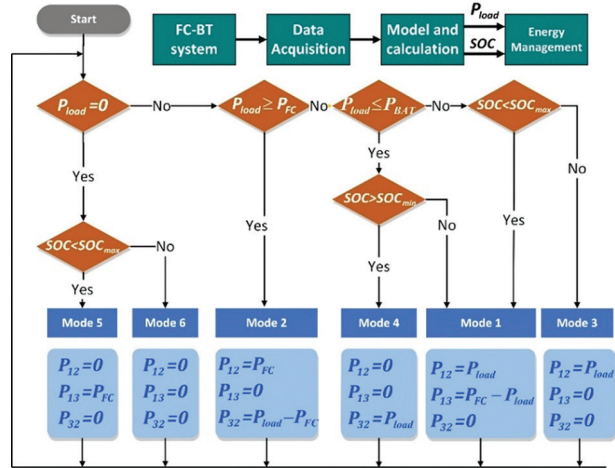


**Fig. 4.** The proposed energy management algorithm

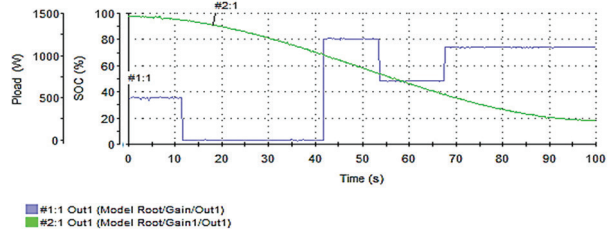


**Fig. 5.** Load power and state of the charge profiles

The comparison between these figures demonstrates the algorithm's accuracy in predicting power distribution under varying loads.

Between 0 and 10 seconds, the load power remains steady at 500 W, demonstrating the system's ability to maintain stable operation under moderate demand conditions. During this period, the battery exceeds its maximum state of charge, and the algorithm effectively directs the battery to supply the required power to the load (mode 4). Between 10 and 30 seconds, with no load demand and the battery is fully charged, the system correctly identifies that no power transfer is needed (mode 6), thereby conserving energy. From 30 to 40 seconds, as the battery's charge level is below its maximum state of charge, the system shifts to charging the battery from the fuel cell, efficiently managing power flow to prepare for future demand. Between 40 and 55 seconds, the fuel cell is delivering the 500W power required by the load (mode 2), highlighting the fuel cell's role in sustaining load demands during periods when the battery is inactive or not available. From 55 to 68 seconds, once again, the battery takes over by supplying the necessary power

to the load (mode 4), showcasing the system's flexibility and its ability to seamlessly switch between power sources depending on the operational needs.

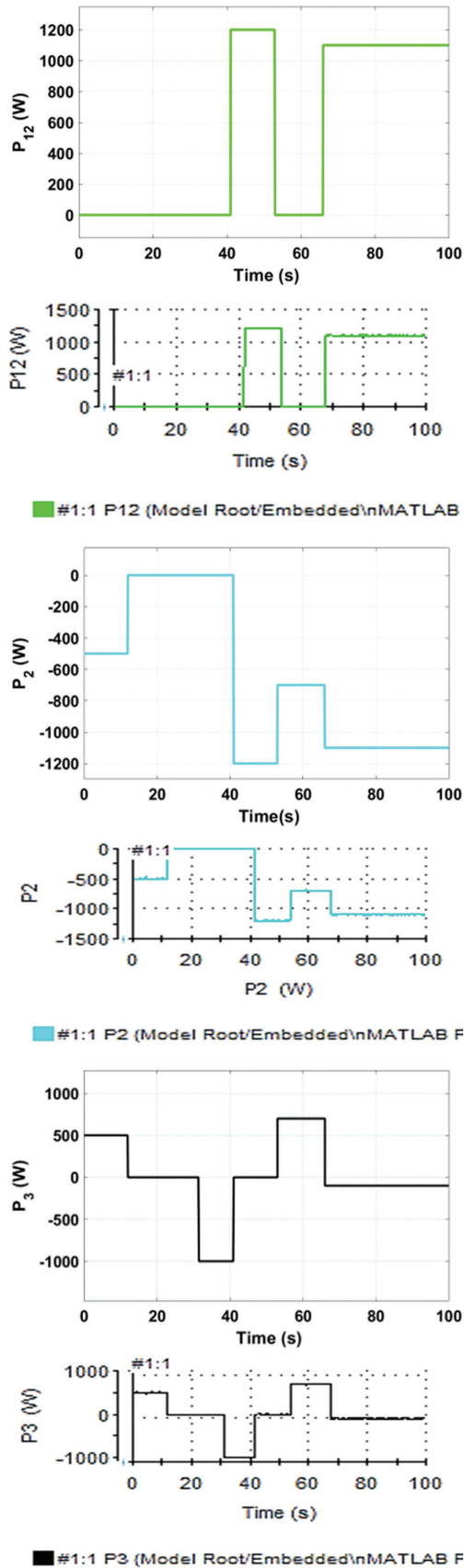


**Fig. 6.** Transferred power between the ports. (a to c) simulation (A to C) Experimental result

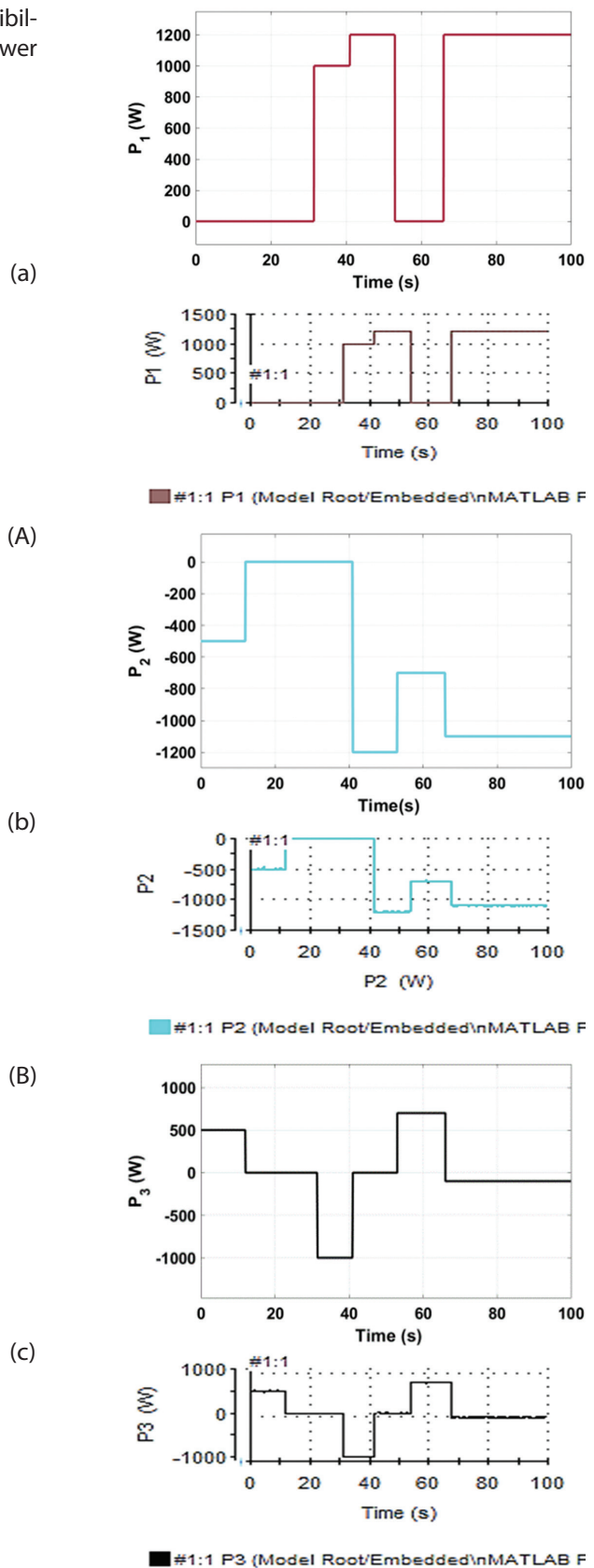


**Fig. 7.** Powers at the ports. (a to c) simulation (A to C) Experimental result

During the period from 68 to 100 seconds, with the battery's charge level dropping below the minimum threshold, the algorithm prioritizes recharging the battery from the fuel cell, while simultaneously ensuring the

load receiving continuous power (mode 1). This operation illustrates the system's capacity for long-term power management, maintaining the battery's health while meeting load requirements.

The close alignment between experimental and simulation results in Figs. 6 and 7 validates the algorithm's robustness and the capability to efficiently supply the required power under various load and state of charge conditions. The proposed algorithm continuously monitors the load power demand, adapting the power flow accordingly. It draws from the battery when the load requires more power than the fuel cell provides and charges the battery with excess power when the load demands less than the fuel cell generates. This strategy ensures optimal power sharing, allowing the fuel cell to operate only when necessary. Consequently, the proposed algorithm proves successful in optimizing power distribution and demonstrating its practicality.

The complexity of the proposed energy management algorithm is notably reduced due to its rule-based optimization approach, which simplifies decision-making processes compared to more complex algorithms such as dynamic programming. This simplicity is advantageous when implementing the algorithm in real-time applications. During experimental tests using the dSPACE 1104 board, the algorithm demonstrated exceptional execution speed, facilitated by the board's rapid sampling capabilities. The dSPACE 1104's high sampling rate, a key characteristic of its design, ensures that the algorithm can continuously monitor and adjust power flow with minimal latency. This rapid processing is crucial for maintaining efficient power management and system stability, particularly in dynamic scenarios where load demands and battery states fluctuate. The rule-based nature of the algorithm further contributes to its efficient execution, as it reduces computational overhead by relying on predefined rules rather than iterative calculations. Overall, the combination of the dSPACE 1104's fast sampling and the algorithm's straightforward structure supports effective real-time performance and reliable operation.

## 5. CONCLUSION

In this paper, we proposed a three-port three-phase DC-DC converter structure tailored for various applications. This structure integrates a fuel cell as the main power source, providing the average power required by the load. Additionally, it includes a battery that functions as a storage device, catering to peak and fluctuating load power demands. An energy management algorithm was also introduced to regulate power flow within the system, ensuring the battery supplies power efficiently to the load.

This strategy not only optimizes power distribution but also highlights the pros of our approach, including improved power sharing and system reliability. However, potential challenges include the complexity of

managing multiple power sources and ensuring seamless transitions between them. Future work could focus on refining the control algorithm and exploring alternative energy storage options to further enhance the system's efficiency and applicability.

## APPENDICES 1: TRANSFORMATION FROM $\Delta$ STRUCTURE TO $T$

$$M_1 = L_m$$

$$M_{12} = \left( \frac{1}{L_m} + \frac{1}{L_{12}} + \frac{1}{L_{31} + L_{23}} \right)^{-1}, M_{13} = \left( \frac{1}{L_m} + \frac{1}{L_{31}} + \frac{1}{L_{12} + L_{23}} \right)^{-1}$$

$$M_2 = n^2 \left( L_m + \left( \frac{1}{L_{12}} + \frac{1}{L_{31} + L_{23}} \right)^{-1} \right), M_{21} = n^2 \left( \frac{1}{L_{21}} + \frac{1}{L_{31} + L_{23}} \right)^{-1} \quad (4)$$

$$M_{23} = n^2 \left( \frac{1}{L_{23}} + \frac{1}{L_{12} + \left( \frac{1}{L_m} + \frac{1}{L_{31}} \right)^{-1}} \right)^{-1}$$

$$M_3 = n^2 \left( L_m + \left( \frac{1}{L_{31}} + \frac{1}{L_{12} + L_{23}} \right)^{-1} \right), M_{31} = n^2 \left( \frac{1}{L_{31}} + \frac{1}{L_{12} + L_{23}} \right)^{-1}$$

$$M_{32} = n^2 \left( \frac{1}{L_{23}} + \frac{1}{L_{31} + \left( \frac{1}{L_m} + \frac{1}{L_{12}} \right)^{-1}} \right)^{-1} \quad (5)$$

$$\Delta M_{12} = M_1 - M_{12}, \quad \Delta M_{13} = M_1 - M_{13}$$

$$L_M = \sqrt{\frac{\Delta M_{12} \Delta M_{13}}{1 - \frac{1}{2} \left( \frac{M_{32}}{M_3} + \frac{M_{23}}{M_2} \right)}}, L_{ext1} = M_1 - L_M \quad (6)$$

$$L_{ext2} = M_2 \left( 1 - \frac{\Delta M_{12}}{L_M} \right), L_{ext3} = M_3 \left( 1 - \frac{\Delta M_{13}}{L_M} \right)$$

Where,

$L_{12}=L_{21}$ : inductance between port 1 and 2 in delta equivalent model.

$L_{13}=L_{31}$ : inductance between port 1 and 3 in delta equivalent model.

$L_{23}=L_{32}$ : inductance between port 2 and 3 in delta equivalent model of the transformer.

$L_{ext1}, L_{ext2}, L_{ext3}$ : inductances of the  $T$  model of the transformer.

$M_{ij}, M_i$ : quantities as functions of  $L_{ij}$  inductances.

$n$ : the turn ratio of the transformer.

$L_m$ : magnetizing inductance in Delta model.

## 6. REFERENCES:

- [1] M. R. Allen, "IPCC Framing and Context", Global Warming of 1.5 °C: IPCC Special Report on Impacts of Global Warming of 1.5°C above Pre-industrial Levels in Context of Strengthening Response to Climate Change, Sustainable Development, and Efforts to Eradicate Poverty", Cambridge University Press, 2022, pp. 49-92.

- [2] BP, "BP Statistical Review of World Energy", <https://www.bp.com/content/dam/bp/business-sites/en/global/corporate/pdfs/energy-economics/statistical-review/bp-stats-review-2021-full-report.pdf> (accessed: 2024)
- [3] S. Farajdadian, A. Hajizadeh, M. Soltani, "Recent developments of multiport DC/DC converter topologies, control strategies, and applications: A comparative review and analysis", *Energy Reports*, Vol. 11, 2024, pp. 1019-1052.
- [4] A. Aouiti, A. Soyed, F. Bacha, "Control and Study of the Bidirectional Three Phase DAB Converter", *Proceedings of the 8th International Conference on Control, Decision and Information Technologies*, Istanbul, Turkey, 17-20 May 2022, pp. 1008-1013.
- [5] A. Aouiti, A. Soyed, F. Bacha, "Study and Control of the  $3\phi$ -DAB DC-DC Converter with a Boost Structure", *Proceedings of the 9th International Conference on Control, Decision and Information Technologies*, Rome, Italy, 2023, pp. 2621-2626.
- [6] R. W. A. A. De Doncker, D. M. Divan, M. H. Kheraluwala, "A three-phase soft-switched high-power-density DC/DC converter for high-power applications", *IEEE Transactions on Industry Applications*, Vol. 27, No. 1, 1991, pp. 63-73.
- [7] S. Yalcin et al. "Experimental analysis of phase shift modulation methods effects on EMI in dual active bridge DC-DC converter", *Engineering Science and Technology*, Vol. 43, 2023, p. 101435.
- [8] J. Yin, X. He, J. Lu, H. S.-H. Chung, "Phase-Shift Control with Unified PWM/PFM for Improved Transient Response in a Bidirectional Dual-Active-Bridge DC/DC Converter", *IEEE Transactions on Industrial Electronics*, Vol. 70, No. 9, 2023, pp. 8862-8872.
- [9] T.-Q. Duong, S.-J. Choi, "Deadbeat Control with Bivariate Online Parameter Identification for SPS-Modulated DAB Converters", *IEEE Access*, Vol. 10, 2022, pp. 54079-54090.
- [10] J. Guacaneme, G. Garcerá, E. Figueres, I. Patrao, R. González-Medina, "Dynamic modeling of a dual active bridge DC to DC converter with average current control and load-current feed-forward", *International Journal of Circuit Theory and Applications*, Vol. 43, 2015, pp. 1311-1332.
- [11] A. Mansour, B. Faouzi, G. Jamel, E. Ismahen, "Design and analysis of a high frequency DC-DC converters for fuel cell and super-capacitor used in electrical vehicle", *International Journal of Hydrogen Energy*, Vol. 39, No. 3, 2014, pp. 1580-1592.
- [12] H. Ataullah et al. "Analysis of the Dual Active Bridge-Based DC-DC Converter Topologies, High-Frequency Transformer, and Control Techniques", *Energies*, Vol. 15, No. 23, 2022, p. 8944.
- [13] F. Slah, A. Mansour, A. Abdelkarim, F. Bacha, "Analysis and design of an LC parallel-resonant DC-DC converter for a fuel cell used in an electrical vehicle", *Journal of Circuits, Systems and Computers*, Vol. 27, No. 8, 2018, p. 1850119.
- [14] A. Aouiti, A. Soyed, F. Bacha, "Study and Analysis of 2-Phase DAB DC-DC Converter for Fuel Cell Applications", *Proceedings of the IEEE International Conference on Advanced Systems and Emergent Technologies*, Hammamet, Tunisia, 29 April - 1 May 2023, pp. 1-6.
- [15] L. Jiang, D. Costinett, "A triple active bridge DC-DC converter capable of achieving full-range ZVS", *Proceedings of the IEEE Applied Power Electronics Conference and Exposition*, Long Beach, CA, USA, 20-24 March 2016, pp. 872-879.
- [16] S. Zou, J. Lu, A. Khaligh, "Modelling and control of a triple-active-bridge converter", *IET Power Electronics*, Vol. 13, No. 5, 2020, pp. 961-969.
- [17] A. Panchbhai, A. Kumar, "Simplified control of TAB converter for scalable multibattery charging system", *International Journal of Circuit Theory and Applications*, Vol. 52, No. 8, 2024, pp. 3797-3816.
- [18] H. Tao, J. L. Duarte, M. A. M. Hendrix, "High-Power Three-Port Three-Phase Bidirectional DC-DC Converter", *Proceedings of the IEEE Industry Applications Annual Meeting*, New Orleans, LA, USA, 23-27 September 2007, pp. 2022-2029.
- [19] H. Tao, J. L. Duarte, M. A. M. Hendrix, "Line-Interactive UPS Using a Fuel Cell as the Primary Source", *IEEE Transactions on Industrial Electronics*, Vol. 55, No. 8, 2008, pp. 3012-3021.
- [20] X. Jun, Z. Xing, Z. Chong-Wei, L. Sheng-Yong, "A novel three-port bi-directional DC-DC converter", *Proceedings of the 2nd International Symposium on Power Electronics for Distributed Generation Systems*, Hefei, China, 16-18 June 2010, pp. 717-720.
- [21] S. Kurm, V. Agarwal, "Interfacing Standalone Loads With Renewable Energy Source and Hybrid Energy Storage System Using a Dual Active Bridge Based Multi-Port Converter", *IEEE Journal of Emerging and Selected Topics in Power Electronics*, Vol. 10, No. 4, 2022, pp. 4738-4748.